Chemical Engineering Journal 146 (2009) 136–142

Contents lists available at ScienceDirect

Chemical Engineering Journal

journal homepage: www.elsevier.com/locate/cej

Steady thermal regimes of a parallel-plane packed bed reactor with an organized structure

Eugen Magyari*

Institut für Hochbautechnik, ETH- Zürich, Wolfgang-Pauli_Str. 1, CH-8093 Zürich, Switzerland

ARTICLE INFO

Article history:
Received 21 April 2008
Received in revised form 8 September 2008
Accepted 9 September 2008

Keywords:
Exothermic reaction
Packed bed reactor
Organized structure
Steady states
Nonlinear model
Analytical solutions

ABSTRACT

The steady conduction regime of exothermic chemical reactions in a packed bed reactor is investigated analytically. A plane-parallel stratification of the reactive granular material is assumed which modulates the rate of the local volumetric heat generation in the reactor. The approach is based on an exactly solvable nonlinear mathematical model which involves two experimentally accessible control parameters, the *intensity parameter* $\lambda > 0$ and *stratification parameter* $s \geq 0$, respectively. In terms of these parameters, the existence domain of the steady temperature solutions and the occurrence of hot spots are discussed. For a given value of the stratification parameter, an upper bound $\lambda_{max}(s)$ of the intensity parameter has been found, such that above of this maximum value of λ the reactor becomes thermally uncontrollable. Below $\lambda_{max}(s)$, unique as well as dual solutions exist. The former ones describe high temperature steady states of the reactor, while the dual solution branches are associated with low and high temperature reaction regimes, respectively. The features of the corresponding temperature distributions are examined in detail.

1. Introduction

The present paper is concerned with parallel-plane packed bed reactors having a *stratified structure* in the transversal direction, and an internal *volumetric heat generation* by exothermic reactions. Model calculations are reported which apply to the *steady conduction regime* of such reactors, encountered in the chemical process engineering, in civil engineering, combustion engineering, thermal explosion control and environmental energy engineering. Specific examples in these fields are the ethanol production from cereals in anaerobic fermenters, hardening of the cement paste of massive concrete members, burning of granular fuels, thermal explosion o fine powders, degradation of organic waste materials in aerobic reactors and natural landfills, etc. Since the temperature and heat transfer control belong to the most important factors in all these processes, a special attention is given in the paper to the occurrence of hot spots [1] and to the upper bounds of the existence domain of steady solutions, [2]. The hot spots due to the excessive fermentation heat generation may decelerate the reaction by killing the yeast in the fermenter (see, e.g. [3]). During the hardening of massive concrete slabs, the hot spots due to the hydration heat release may lead to early-age thermal stresses. This may cause cracking, which in turn reduces the durability of highly expensive structures, [4–6]. In rapid-hardening cement-based fiber composites, e.g. adiabatic temperature maxima up to 140 °C have been measured, [7]. In combustion processes of fine granular materials, by contrast, where the overrunning of the *ignition temperature* is a necessary condition of the steady evolution, the occurrence of hot spots is a desired phenomenon. The upper limits of the existence domain of steady solutions represent in these processes the regime above of which the reactor becomes uncontrollable and thermal explosion occurs (see e.g. [8]).

Comparing to the classical literature on the *conduction regime* of parallel-plane packed bed reactors (see, e.g. [8] and [9]), the contribution of the present paper consists of the inclusion in the mathematical model of an *organized structure*, a *stratification* of the reactive granular material, which in turn modulates the rate of the local volumetric heat generation. In a hardening concrete slab, e.g. the plane-parallel stratification implies a gradual variation of the water/cement ratio with the transversal coordinate and, consequently, a variation of the heat released by hydration. The effect of such type of stratification on the possible steady temperature profiles of the packed bed reactors is discussed in the paper in some detail.

2. Basic equations and problem formulation

We consider a packed bed reactor with parallel-plane boundaries which are kept at the same constant temperature T_0. Be $2L$ the distance between the boundaries. The x-axis is perpendicular to

* Tel.: +41 61 731 38 46.
E-mail addresses: magyari@hbt.arch.ethz.ch, magyari@bluewin.ch.

1385-8947/$ – see front matter © 2008 Elsevier B.V. All rights reserved.
doi:10.1016/j.cej.2008.09.005

Nomenclature

c	specific heat (J/kg K)
E_a	activation energy (J)
k	thermal conductivity (W/m K)
k_B	Botzmann constant (1.38×10^{-23} J/K)
K	integration constant
K_*	threshold value e^s of K
$\tilde{K}_*$	dual counterpart of K
L	half-thickness of packed bed (m)
q	dimensionless wall heat flux
Q	rate of volumetric heat generation (W/m^3)
Q_{tot}	dimensionless rate of total heat release
Q_{local}	dimensionless rate of local heat release
s	stratification parameter
t	time variable (s)
T	absolute temperature (K)
T_0	boundary temperature (K)
W	dimensionless function ($W = \theta + sX$)
x	dimensional transversal coordinate (m)
X	dimensionless transversal coordinate ($X = x/L$)
X_0	integration constant

Greek symbols

α	constant (K^{-1}) $\alpha = E_a/(k_B T_0^2)$
λ	intensity parameter
Λ	dimensionless structure function of stratification ($\Lambda = \lambda\, e^{sX}$)
ρ	density (kg/m^3)
θ	dimensionless temperature, $\theta = \alpha(T - T_0)$

Subscripts

*	related to threshold value of K
max	related to maximum value of λ

the boundaries located at $x = -L$ and $x = +L$, respectively (see Fig. 1). The reactor is filled with the mixture of a fine granular material of which composition varies with the x-coordinate continuously. We assume that in this *organized structure* an exothermic chemical or biochemical reaction occurs, such that the rate of the volumetric heat generation is a continuous function both of the local temperature T and the coordinate x. The temperature field $T = T(x,t)$ in this parallel-plane reactor is governed by the Fourier equation

$$\rho c \frac{\partial T}{\partial t} = k \frac{\partial^2 T}{\partial x^2} + Q(x, T) \tag{1}$$

where $Q(x,T)$ is the rate of volumetric heat generation by the exothermic reaction and is everywhere positive. We further assume that the density ρ, the specific heat c and the thermal conductivity k of the material are slowly varying functions of the coordinate x and of reaction time t, such that all of them may be considered as constants.

As it is well known, the heat generated by the exothermic reaction increases in turn the reaction velocity itself, and thus it enhances the rate of heat generation continuously (positive feedback). This phenomenon is described by the Arrhenius law, which implies that the source term $Q(x,T)$ of Eq. (1) has the form

$$Q(x, T) = Q_0(x)\ e^{-(E_a/k_B T)} \tag{2}$$

Here $E_a > 0$ is the activation energy of the reaction and k_B the Boltzmann constant. Assuming that the temperature inside the reactor do not differs substantially from the wall temperature T_0, in the exponential of Eq. (2), $1/T$ can be expanded in a Taylor series of the temperature difference $T - T_0$ and, as shown already by Frank-Kamenetzkii [9], the first order approximation $1/T \cong 1/T_0 - (T - T_0)/T_0^2$ may be applied. Thus, Eq. (2) becomes

$$Q(x, T) = \tilde{Q}_0(x)\ e^{\alpha(T - T_0)} \tag{3}$$

where $\tilde{Q}_0(x) = Q_0(x) \exp(-E_a/k_B T_0) > 0$ and $\alpha = E_a/(k_B T_0^2) > 0$.

The thermal evolution of the reactor is determined by the balance of the heat generated by the exothermic reaction and the heat extracted through the walls which are kept at the lower temperature T_0 (isothermal wall cooling). The latter process depends obviously on the thermal conductivity and the heat storage capacity of the reacting material. When over the heat outflow process the heat generation dominates, the temperature of the reactor increases uncontrollably. Accordingly, in the industrial practice one is interested to reach a time-independent (steady) working regime of the reactor in which between the generated and extracted heat flows an exact balance holds. In our present model, the temperature field $T = T(x)$ of this steady regime is governed by the two-point boundary value problem

$$k \frac{\mathrm{d}^2 T}{\mathrm{d}x^2} + \tilde{Q}_0(x)\ e^{\alpha(T - T_0)} = 0, \quad T(-L) = T(L) = T_0 \tag{4}$$

Now, introducing the dimensionless coordinate X and the dimensionless temperature θ by the definitions $X = x/L$, $\theta(X) = \alpha(T - T_0)$, Eq. (4) becomes

$$\frac{\mathrm{d}^2 \theta}{\mathrm{d}X^2} + \Lambda(X)\ e^{\theta} = 0, \quad \theta(-1) = \theta(1) = 0 \tag{5}$$

where the notation $\Lambda(X) = \alpha\ L^2\ \tilde{Q}_0(x)/k > 0$ has been used. The dimensionless function $\Lambda(X)$ describes the way in which the structure of the packed bed is organized with respect to local intensity $\tilde{Q}_0(x)$ of the heat generation. In order to be specific, in the present model calculations we assume that the structure exhibits a *plane-parallel stratification* described by the exponential law

$$\Lambda(X) = \lambda\ e^{sX} \tag{6}$$

Here λ and s are the *control parameters* of our engineering problem. The *intensity parameter* λ is necessarily positive (exothermic reactions), while the parameter s which characterizes the stratification of the reacting material in the packed bed, may be positive, negative or zero. Hence, for a given λ, the intensity of the volumetric heat

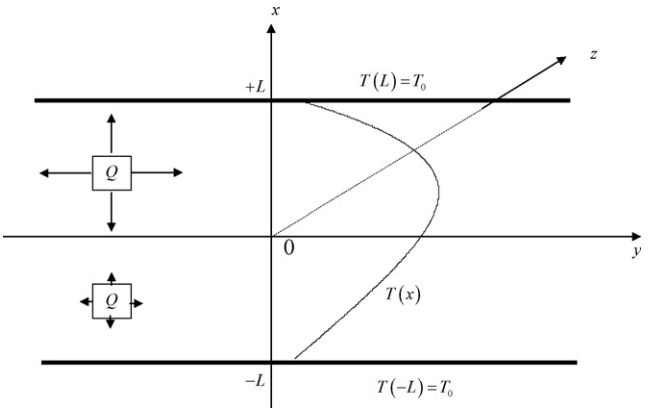

Fig. 1. Schematic representation of the parallel-plane reactor with coordinate system, volumetric heat generation $Q(X)$, isothermal boundary conditions $T(\pm L) = T_0$ and a typical asymmetric temperature distribution $T(x)$. Due to the stratified structure of the reactive material in the x-direction, the rate of the volumetric heat generation $Q(x)$ depends on the x coordinate explicitly and, in spite of the symmetric boundary conditions $T(\pm L) = T_0$, the temperature profiles $T(x)$ are asymmetric with respect to the midplane of the reactor.

sources increases or decreases with increasing value of X when the *stratification parameter* s is positive or negative, respectively. However, taking into account that the boundary value problem (5), (6) is invariant under the transformations ($X \to -X$, $s \to -s$), it is sufficient to consider only the non-negative values of the stratification parameter s, without any lost of generality. The vanishing value of s corresponds to $\Lambda(X) = \lambda = \text{constant}$, i.e. to a uniform distribution of the heat sources in the (non-stratified) reactor. This latter case of the two-point boundary value problem (5) has already been investigated and solved by Frank-Kamenetzkii [9], as well as by Agarwal and Loi [10] as a specific example in the context of nth order multipoint boundary value problems. We also mention here that some special solutions of the problem (5) have been given recently by Goyal [11] which, however, correspond to the case $\Lambda(x) < 0$ and thus do not apply to our present issue.

3. Solution

Changing in Eq. (5), with $\Lambda(X)$ is given by Eq. (6), from θ to the new dependent variable W by the substitution $\theta(X) = W(X) - sX$, the problems (5) and (6) becomes

$$\frac{d^2W}{dX^2} + \lambda e^W = 0, \qquad W(\pm 1) = \pm s \tag{7}$$

One immediately sees that the first Eq. (7) admits the first integral

$$\left(\frac{dW}{dX}\right)^2 = 2\lambda(K - e^W) \tag{8}$$

where K is a constant of integration. This equation can easily be integrated, yielding

$$e^{-(W/2)} = \frac{1}{\sqrt{K}} \cosh\left[\sqrt{\frac{\lambda K}{2}}(X - X_0)\right] \tag{9}$$

where X_0 is the second integration constant. On account of $W = \theta + sX$, Eq. (9) gives for the (dimensionless) temperature field the expression

$$\theta(X) = -\ln\left(\frac{e^{sX}}{K} \cosh^2\left[\sqrt{\frac{\lambda K}{2}}(X - X_0)\right]\right) \tag{10}$$

The boundary conditions $\theta(-1) = \theta(1) = 0$ yield for the determination of the integration constants K and X_0 in terms of λ and s the system of transcendental equations

$$\cosh\left[\sqrt{\frac{\lambda K}{2}}(1 + X_0)\right] = \sqrt{K e^s}, \quad \cosh\left[\sqrt{\frac{\lambda K}{2}}(1 - X_0)\right] = \sqrt{K e^{-s}} \tag{11}$$

A simple inspection of this system of equations shows that it admits real solutions only when, for a given s, K is equal to, or larger than a threshold value K_*, namely

$$K \geq K_* = e^s \tag{12}$$

In addition to the temperature field (10), further quantities of physical and engineering interest are the (dimensionless) heat fluxes $q(\pm 1) = -\theta'(\pm 1)$ through the plane boundaries of the reactor at $X = \pm 1$ (the prime denote differentiation with respect to X), as well as the (dimensionless) rate of total heat release by the exothermic reactions

$$Q_{tot} = \int_{-1}^{1} (\lambda e^{sX+\theta})\, dX \tag{13}$$

Table 1
In the first six rows the coordinates of the threshold points (K_*, λ_*) and of the maxima (K_{max}, λ_{max}) of the curves $\lambda = \lambda(K; s)$ plotted in Fig. 2a, as well as the corresponding values of the integration constant X_0 are included. The last two rows refer to the dual right-branch counterparts ($\tilde{K}_*$, λ_*; $\tilde{X}_{0,*}$) of the (left-branch) threshold points (K_*, λ_*; $X_{0,*}$) included in rows 1–3.

s	0	0.7	1	1.5	1.8	2
K_*	1	2.01375	2.71828	4.48169	6.04965	7.38906
λ_*	0	0.435818	0.505311	0.530426	0.510891	0.489117
$X_{0,*}$	0	1	1	1	1	1
K_{max}	3.27672	3.82685	4.44598	6.17899	7.78815	9.17882
λ_{max}	0.878453	0.832866	0.788743	0.693054	0.627893	0.583216
$X_{0,max}$	0	0.330829	0.448318	0.602272	0.671772	0.710162
$\tilde{K}_*$	∞	23.3089	17.4406	15.2799	16.0226	17.1377
$\tilde{X}_{0*}$	0	0.159063	0.246800	0.392276	0.471786	0.520005

Bearing in mind Eqs. (10) and (11), one obtains for the above quantities the expressions

$$q(-1) = s - \sqrt{2\lambda(K - e^{-s})}, \quad q(1) = s + \sqrt{2\lambda(K - e^s)}, \tag{14}$$

$$Q_{tot} = \sqrt{2\lambda}\left(\sqrt{K - e^s} + \sqrt{K - e^{-s}}\right) \tag{15}$$

Obviously, $Q_{tot} = q(1) - q(-1)$, in full agreement with our physical expectation and the integral of the energy balance Eq. (5) with respect to X from -1 to 1.

4. Discussion

The basic task is now to determine the real solutions (K,X_0) of the system of Eq. (11) for specified values of the control parameters $s \geq 0$ and $\lambda > 0$. Unfortunately, the system (11) does not admit an explicit solution for K and X_0, but only for λ and X_0 in terms of s and K which reads

$$\lambda = \frac{1}{2K}\left(\operatorname{arccosh}\sqrt{K e^s} + \operatorname{arccosh}\sqrt{K e^{-s}}\right)^2 \tag{16}$$

$$X_0 = \frac{\operatorname{arccosh}\sqrt{K e^s} - \operatorname{arccosh}\sqrt{K e^{-s}}}{\operatorname{arccosh}\sqrt{K e^s} + \operatorname{arccosh}\sqrt{K e^{-s}}} \tag{17}$$

where $\operatorname{arccosh}(z) = \ln\left(z + \sqrt{z^2 - 1}\right)$.

The values of λ and X_0 corresponding to the threshold value (12) of K are

$$\lambda_* = 0 \quad \text{and} \quad X_0^* = 0 \quad \text{for } s = 0, \qquad \lambda_* = \frac{1}{2} e^{-s} \operatorname{arccosh}^2 e^s \quad \text{and}$$
$$X_0^* = 1 \quad \text{for } s \neq 0 \tag{18}$$

In Fig. 2a and b, λ and X_0 given by Eqs. (16) and (17) are plotted as functions of K for the values $s = 0$, 0.7, 1, 1.5, 1.8 and 2 of the stratification parameter. The dots mark in these figures the values of λ_* and X_0^* given by Eq. (18), and the dotted curve of Fig. 2a represents the envelope

$$\lambda_* = \frac{1}{2K_*} \operatorname{arccosh}^2 K_* \tag{19}$$

of the threshold points (K_*, λ) in the plane (K, λ). The maximum of the envelope (19) is $(\lambda_*)_{max} = 0.532222$, being reached at $K_* = 4.00737$, i.e. at the value $s = \ln(4.00737) = 1.38814$ of the stratification parameter. The threshold values (K_*, λ_*; X_{0^*}), as well as the values (K_{max}, λ_{max}; X_{0max}) associated with the maxima of the curves $\lambda = \lambda(K;s)$ of Fig. 2a are collected in the first six rows of Table 1. As suggested by Fig. 2a and b, all three functions λ, λ_* and X_0 approach zero as $K \to \infty$. More precisely, to the leading order, the following asymptotic behaviors hold

$$\lambda \sim \frac{\ln^2(4K)}{2K}, \quad \lambda_* \sim \frac{\ln^2(2K)}{2K}, \quad X_0 \sim \frac{s}{\ln(4K)} \quad \text{as } K \to \infty \tag{20}$$

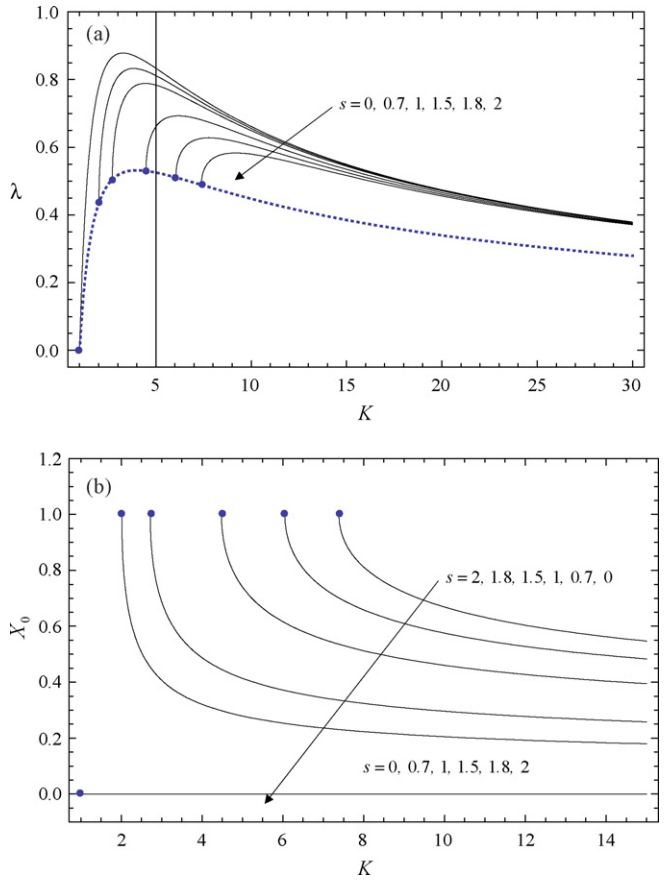

Fig. 2. (a) The solid curves show of the intensity parameter λ as a function of the integration constant K for six specified values of the stratification parameter s (see also Table 1). The dotted curve represents the envelope of the points corresponding to the threshold values $K_* = e^s$ of K. The maximum of the envelope $(\lambda_*)_{max} = 0.532222$ is reached at $K_* = 4.00737$. (b) Plot of X_0 as a function of K according to Eq. (17), for six specified values of the stratification parameter s. The dots mark the values $X_0 = 0$ and $X_0 = 1$ corresponding to the threshold values $K_* = e^s$ of K for $s = 0$ and $s \neq 0$, respectively, according to Eq. (18).

The main message of Fig. 2a is that for any given value $s \geq 0$ of the stratification parameter, a maximum value $\lambda_{max}(s)$ of the intensity parameter λ exists such that above of this *upper bound* no steady temperature solutions are possible. The domain of existence of the solutions is the finite λ-range

$$0 < \lambda \leq \lambda_{max}(s) \quad \text{for all } s \geq 0 \tag{21}$$

and consists of a left- and a right-branch of the curve λ, which match at $\lambda = \lambda_{max}(s)$. The maximum of λ corresponding to $s = 0$ represents the *absolute maximum* of all the λ-cures

$$\lambda_{\max}(0) > \lambda_{\max}(s) \quad \text{for all } s > 0 \tag{22}$$

As recognized already by Frank-Kamenetskii [9] and by Agarwal and Loi [10], in the case of homogeneous reactor ($s = 0$), for every given value of λ in the range $0 < \lambda < \lambda_{max}(0)$ two independent solutions (dual solutions) exist which become coincident as $\lambda \to \lambda_{max}(0)$. These solutions correspond according to Eqs. (17) and (16) to the same value $X_0 = 0$ of the integration constant X_0 (see Fig. 2b), but to two different values K_1 and $K_2 > K_1$ of the constant K, which are obtained as solutions of the transcendental equation

$$\lambda = \frac{2}{K}\operatorname{arccosh}^2\sqrt{K}, \quad 0 < \lambda < \lambda_{max}(0), \tag{23}$$

The corresponding left-branch ("1") and right-branch ("2") temperature solutions (10)

$$\theta_{1,2}(X) = -2\ln\left[\frac{\cosh\left(X\operatorname{arcosh}\sqrt{K_{1,2}}\right)}{\sqrt{K_{1,2}}}\right] \quad (s = 0) \tag{24}$$

are symmetric with respect to the midplane $X = 0$ of the reactor.

Although the domain of existence of the steady solutions given by Eq. (21) is formally the same for both $s = 0$ and $s \neq 0$, in the later case of the stratified reactor an essential new feature occurs. Indeed, in the range between $\lambda = 0$ and the λ-value (19) corresponding to the threshold value (12) of K,

$$0 < \lambda < \lambda_* = \frac{e^{-s}}{2}\operatorname{arccosh}^2(e^s) \quad (s \neq 0) \tag{25}$$

the steady temperature solution (10) for the stratified reactor is always *unique*, while in the case $s = 0$, no unique solutions exist at all (except for the coincident solutions at $\lambda = \lambda_{max}(0)$). Then, in the range $\lambda_* \leq \lambda \leq \lambda_{max}(s)$ dual left- and right-branch solutions occur which also become coincident as $\lambda \to \lambda_{max}(s)$.

Concerning the dual solutions, between the cases $s = 0$ and $s \neq 0$ an essential deviation is encountered again. While in the case $s = 0$, the constant of integration X_0 is vanishing for all λ-values in the range (21) (which implies that for $s = 0$ all the dual solutions are symmetric with respect to the midplane $X = 0$ of the reactor), in the case $s \neq 0$ the dual solutions are always non-symmetric, being associated with different non-vanishing values of X_0 (see also Table 1). To be more specific in discussing the features of the solution space in the case of stratified reactor, let us inspect Fig. 3, where the λ-curve of Fig. 2a corresponding to $s = 1$ of has been picked out as a representative example for all cases with $s \neq 0$.

The dual left- and right-branch solutions are obtained in this case in the interval $0.505311 \leq \lambda \leq 0.788743$, while the unique right-branch solutions from the λ-range $0 < \lambda < 0.505311$ emerge. In Fig. 4, four temperature profiles (10) related to Fig. 3 are shown. θ_1 and θ_2 are the dual left- and right-branch solutions associated with the threshold point $(K_*, \lambda_*; X_{0,*})$ and with its counterpart $(\tilde{K}_*, \lambda_*; \tilde{X}_{0,*})$ corresponding to the same $\lambda = \lambda_*$, respectively (see also Table 1). θ_3 represents the coincident dual solutions corresponding to the maximum $(K_{max}, \lambda_{max}; X_{0,max})$ of the λ-curve of Fig. 3, and the temperature profile θ_4 represents the unique right-branch solution associated with the value $\lambda_4 = 0.4 < \lambda_*$ of the intensity parameter, the corresponding K and X_0 values being $K_4 = 27.1034$ and $X_{0,4} = 0.219622$, respectively. It is clearly seen that all these temperature profiles are non-symmetric with respect to the midplane. Fig. 4 also shows that the left-branch solutions describe low tem-

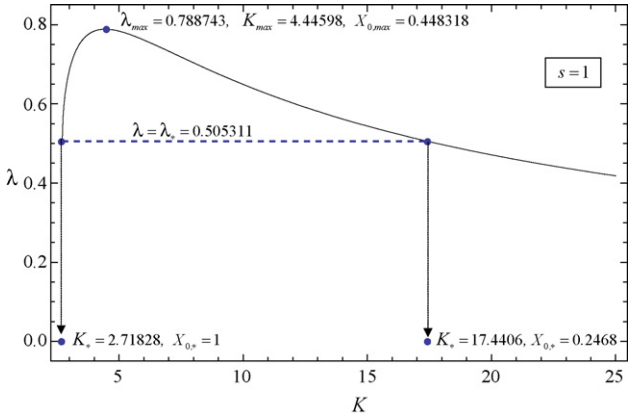

Fig. 3. Existence domain of the steady solutions (10) for $s = 1$, as a representative for the reactor with stratified structure, $s \neq 0$.

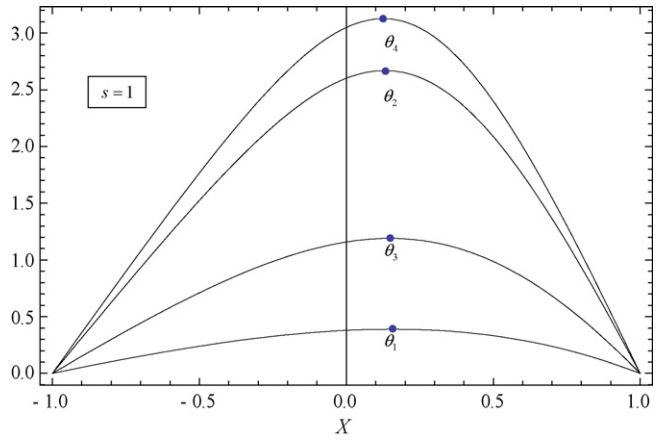

Fig. 4. Four steady temperature profiles related to Fig. 3. θ_1 and θ_2 are the dual left- and right-branch solutions associated with the (left-branch) threshold point (K_*, λ_*; $X_{0,*}$) and its right-branch counterpart ($\tilde{K}_*$, λ_*; $\tilde{X}_{0,*}$) corresponding to the same $\lambda = \lambda_*$, respectively. θ_3 represents the coincident dual solutions corresponding to the maximum (K_{max}, λ_{max}; $X_{0,max}$) and the temperature profile θ_4 represents the unique right-branch solution associated with the value $\lambda_4 = 0.4 < \lambda_*$ of the intensity parameter The dots marks the maxima of the profiles θ (see also Table 2).

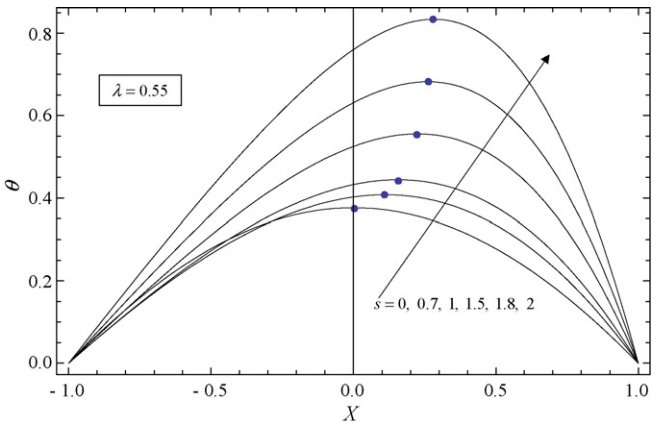

Fig. 5. Left-branch temperature profiles plotted as functions of X for the same value $\lambda = 0.55$ of the intensity parameter and six different values of the stratification parameter s. The maxima θ_{max}, marked by dots, and the other characteristic values associated with these temperature distributions are collected in Table 3.

Table 3
Characteristic values of the left-branch temperature profiles θ shown in Fig. 5.

s	0	0.7	1	1.5	1.8	2
K	1.45720	2.07140	2.73299	4.48918	6.11218	7.68656
X_0	0	0.776877	0.915206	0.963221	0.921716	0.862898
X_{max}	0	0.111672	0.156703	0.225303	0.261467	0.282535
θ_{max}	0.376518	0.40792	0.444278	0.555568	0.682058	0.833695
$q(1)$	0.70917	0.951821	1.12723	1.59076	2.06227	2.57206
Q_{tot}	1.41834	1.56799	1.74019	2.25701	2.81992	3.45413
$Q_{local,max}$	0.801461	1.13927	1.50315	2.46905	3.36169	4.22761

perature and the right-branch solutions, high-temperature regimes (*hot spots*) of the exothermic reactions, respectively. The abscissa X_{max} of the maxima, and the maxima θ_{max} of the temperature profiles (10) are given by

$$X_{max} = X_0 - \sqrt{\frac{2}{\lambda K}}\ \operatorname{arctanh}\left(\frac{s}{\sqrt{2\lambda K}}\right), \tag{26}$$

$$\theta_{max} = \ln K + \ln\left(1 - \frac{s^2}{2\lambda K}\right) - s X_{max} \tag{27}$$

For the homogeneous reactor, Eqs. (26) and (27) reduce to

$$X_{max} = 0, \quad \theta_{max} = \ln\ K \quad (s = 0) \tag{28}$$

Thus, for the stratified reactor ($s \neq 0$) the value of X_{max} is a measure of the deviation of temperature profile from the symmetric shape corresponding to the homogeneous structure.The characteristic values λ, K, X_0, X_{max}, θ_{max} and Q_{tot} of the temperature distributions shown in Fig. 4 are collected in Table 2. Already a simple inspection of Table 2 suggests that the increasing values of the temperature maxima are correlated with increasing values of K. Thus, the rate of heat generation Q_{tot} increases with increasing values of θ_{max}. At the same time, both X_0 and X_{max} decrease with increasing values of θ_{max}. For $K \gg 1$ all these features can also be proved analytically. Indeed, bearing in mind the third Eq. (20) and expanding Eqs. (26) and (27) for large values of K, we obtain to the leading order the simple expressions

$$X_{max} = \frac{s}{\ln(4K)}, \quad \theta_{max} = \ln K \quad (K \gg 1) \tag{29}$$

which prove the above statement. To the order $1/K$, the more accurate approximation formulas

$$X_{max} = \frac{s}{\ln(4K)} - \frac{s}{\lambda K} \quad (K \gg 1) \tag{30}$$

and

$$\theta_{max} = \ln K - \frac{s^2}{\ln(4K)} + \frac{s^2}{2\lambda K} \quad (K \gg 1) \tag{31}$$

result. For the high temperature profiles θ_2 and θ_4 of Fig. 4, e.g. Eq. (31) approximates the corresponding exact results of Table 2 with an accuracy of 0.4% and 0.2%, respectively.

All the temperature profiles shown in Fig. 4 correspond to the same value $s = 1$ of the stratification parameter. In odder to illustrate the dependence of the steady temperature distributions on the parameter s, in Fig. 5 the left-branch temperature profiles have been plotted as functions of X for the same value $\lambda = 0.55$ of the intensity parameter and the six different values of s considered in Fig. 2a and b. The characteristic values associated with these temperature distributions are collected in Table 3.

Fig. 5 and Table 3 show that for the left-branch solutions considered, both the maximum temperature θ_{max} and its coordinate X_{max} increase with increasing values of the stratification parameter s. Similarly, the rate of total reaction heat release Q_{tot}, as well as the heat flux $q(1)$ increase with increasing values of s, in full agreement

Table 2
Characteristic values of the four temperature profiles θ corresponding to $s = 1$ and shown in Fig. 4. The functions θ are listed in table according to the increasing values of their maxima θ_{max} (the bottom-up sequence in Fig. 4).

θ	λ	K	X_0	X_{max}	θ_{max}	Q_{tot}	*Note*
θ_1	0.50531	2.71828	1	0.15729	0.39013	1.54122	Dual solution to θ_2
θ_3	0.78874	4.44598	0.44832	0.14831	1.18986	4.18725	Coincident dual solutions at $\lambda = \lambda_{max}$
θ_2	0.50531	17.4406	0.24680	0.13111	2.66929	8.0111	Dual solution to θ_1
θ_4	0.4	27.1034	0.21962	0.12592	3.12652	9.04156	Unique solution

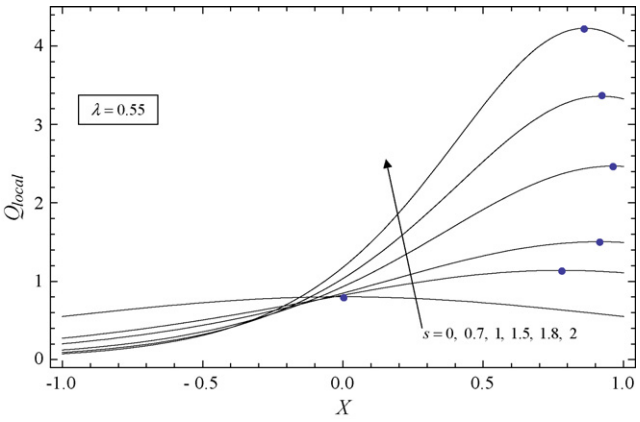

Fig. 6. The rate of local reaction heat release $Q_{local}(X)$ plotted as function of X the left-branch temperature profiles shown in Fig. 5. The dots mark the maximum values $Q_{local,max}$ included in the last row of Table 3.

with our physical expectation. It is also instructive to calculate, in addition to Q_{tot}, the rate of the local reaction heat release $Q_{local}(X)$, which represents the integrand in Eq. (13) of Q_{tot}, i.e.

$$Q_{local}(X) = \lambda\, e^{sX+\theta(X)} \tag{32}$$

Bearing in mind Eq. (10), one easily obtains for Q_{local} the explicit expression

$$Q_{local}(X) = \frac{\lambda K}{\cosh^2[\sqrt{(\lambda K/2)}(X - X_0)]} \tag{33}$$

One immediately sees that $Q_{local}(X)$ reaches at $X = X_0$ its maximum value

$$Q_{local,max} = \lambda K \quad (X = X_0) \tag{34}$$

The values of $Q_{local,max}$ are included in the last row of Table 3 and $Q_{local}(X)$ given by Eq. (33) is plotted for $\lambda = 0.55$ and $s = 0$, 0.7, 1, 1.5, 1.8 and 2 in Fig. 6.

Comparing Figs. 5 and 6 one sees that the coordinate X_{max} of θ_{max} coincides with the coordinate X_0 of $Q_{local,max}$ only for the non-stratified reactor ($s = 0$), in which case $X_{max} = X_0 = 0$, and both functions $\theta(X)$ and $Q_{local}(X)$ are symmetric with respect to the midplane $X = 0$. In the stratified reactor however, both these symmetries get broken, i.e. $X_{max} \neq 0$ and $X_0 \neq 0$. Moreover, X_0 is shifted with respect to X_{max} to the right (se also Table 3). Indeed, according to Eq. (26) one has

$$X_0 - X_{\max} = \sqrt{\frac{2}{\lambda K}}\ \operatorname{arctanh}\left(\frac{s}{\sqrt{2\lambda K}}\right) > 0 \quad \text{for } s > 0 \tag{35}$$

In other words, as an effect of stratification ($s \neq 0$), the maximum of the steady temperature profiles (10) is "retarded" with respect to the maximum of the rate $Q_{local}(X)$ of local heat release by exothermic reactions. This (nonlinear) effect becomes manifest already by a simple inspection of Eq. (32).

5. Summary and conclusions

The steady conduction regime of a parallel-plane packed bed reactor with a stratified structure and internal volumetric heat generation by exothermic reactions has been investigated. The approach was based on an exactly solvable one-dimensional nonlinear mathematical model which involves two experimentally accessible control parameters, the intensity parameter λ and stratification parameter s. From engineering point of view, this model corresponds to a three dimensional reactor whose y- and z-dimensions are much larger than the x dimension, i.e. than the distance $2L$ between the two plane boundaries (Fig. 1). In this case the finite-size effects in y- and z-directions of the real reactor can be neglected, and the results of the (mathematically) one-dimensional model calculations hold in the three dimensional world as well. The intensity parameter λ is an intrinsic material constant which is determined by the reaction heat. The stratification parameter s is rather a geometrical characteristic which is determined by the way in which the structure of the reacting materials has been organized between the plane boundaries. Since the problem possesses a natural left–right symmetry, the positive and negative values of s are trivially equivalent. The stratification factor e^{sX} increases/decreases from the lower to the upper boundary monotonically when s is positive/negative (Fig. 1). The central issue of the paper was to investigate the effect of the organized structure of the reactive granular material on the heat release by the exothermic reactions and on the possible steady temperature distributions when the boundaries of the reactor are kept at the same constant temperature. The main results of the paper can be summarized as follows.

1. For every given value of the stratification parameter $s \geq 0$, an upper bound $\lambda_{max}(s)$ of the intensity parameter has been found, such that above of this maximum value of λ no steady temperature solution exists, i.e. the reactor becomes thermally uncontrollable. The absolute maximum of λ is obtained for $s = 0$, i.e. $\lambda_{max}(0) > \lambda_{max}(s)$ for all $s > 0$.
2. While in the homogeneous (non-stratified) reactor, below λ_{max} only dual solutions exist, in the stratified structure ($s > 0$) both unique and dual solutions are possible. The unique solutions always describe high temperature steady states (hot spots) of the reactor, while the dual solution branches are associated with low and high temperature reaction regimes, respectively.
3. Whereas in the homogeneous reactor the steady temperature filed $\theta(X)$ as well as the rate of local heat release $Q_{local}(X)$ always are symmetric functions with respect to the midplane $X = 0$, in the stratified case the symmetries of both these functions get broken (see Figs. 5 and 6). The maximum of the asymmetric temperature profiles is shifted (for positive s) toward the upper boundary. This feature is due to the fact that with increasing values of X, the stratification factor e^{sX} of the source term increases, too. On this reason the asymmetry of the temperature profiles is physically expected. However, it is quite surprising that the local reaction heat release $Q_{local}(X)$ plotted in Fig. 6 does not increase everywhere, but possesses a maximum in the neighborhood of the upper boundary. This is not obvious from the very beginning since it is the joint effect of the boundary conditions on the one hand, and of a subtle nonlinear interplay of the explicit X-dependence via e^{sX} and of the implicit X-dependence via $\theta(X)$ present in the expression $Q_{local}(X) = \lambda e^{sX+\theta(X)}$ of the local reaction heat release, on the other hand.

We may conclude that the stratification exerts a substantial influence on the steady conduction regime of the reactor. This circumstance has important consequences for all the practical applications of the model. Moreover, the range of validity of the above model calculations extends also to the case of fluidized beds as long as the thermal diffusion is the governing internal heat transfer phenomenon compared to the convection. Since in this regime of the fluidized beds no convective instabilities can occur, the investigation of a possible crossover between the low and high temperature conduction regimes under the influence of small perturbations is a challenging research objective.

References

[1] E.J. Westernik, N. Koster, K.R. Westerterp, The choice between cooled tubular reactor models: analysis of the hot spot, Chem. Eng. Sci. 45 (1990) 3443–3455.
[2] C.-H. Li, B.A. Finlayson, Heat transfer in Packed bed. A reevaluation, Chem. Eng. Sci. 32 (1977) 1055–1066.
[3] J.H.T. Luong, B. Volesky, A new technique for continuous measurement of heat of fermentation, Eur. J. Appl. Microbiol. Biotechnol. 16 (1982) 28–34.
[4] F.-J. Ulm, O. Coussy, Strength growth as chemo-plastic hardening in early age concrete, ASCE J. Eng. Mech. 122 (1996) 1123–1132.
[5] G. DeSchutter, Fundamental study of early-age concrete behavior as a basis for durable concrete structures, Mater. Struct. 35 (2002) 15–21.
[6] C.V. Nielson, A. Berrig, Temperature calculations during hardening, Concrete Int. 27 (2005) 73–76.
[7] P. Frantzis, Effect of early-age temperature rise on stability of rapid-hardening cement fiber composites, ASCE J. Mater. Civil Eng. 18 (2006) 568–575.
[8] P. Gray, P.R. Lee, Thermal explosion theory, Oxid. Combust. Rev. 2 (1967) 3–183.
[9] D.A. Frank-Kamenetskii, Diffusion and Heat Exchange in Chemical Kinetics, Plenum Press, New York, 1969.
[10] R.P. Agarwal, S.L. Loi, On approximate Piccard's iterates for multipoint boundary value problems, Numer. Anal. 8 (1984) 381–391.
[11] V. Goyal, On a second order nonlinear boundary value problem, Appl. Math. Lett. 19 (2006) 1406–1408.